

# Number counts and dynamical vacuum cosmologies

N. Chandrachani Devi,<sup>1</sup> H. A. Borges,<sup>2,3</sup> S. Carneiro<sup>2</sup> and J. S. Alcaniz<sup>1\*</sup>

<sup>1</sup>*Observatório Nacional, 20921-400 Rio de Janeiro, RJ, Brazil*

<sup>2</sup>*Instituto de Física, Universidade Federal da Bahia, 40210-340 Salvador, BA, Brazil*

<sup>3</sup>*Institute of Cosmology and Gravitation, University of Portsmouth, Portsmouth PO1 3FX, UK*

Accepted 2014 December 15. Received 2014 December 3; in original form 2014 July 7

## ABSTRACT

We study non-linear structure formation in an interacting model of the dark sector of the Universe in which the dark energy density decays linearly with the Hubble parameter,  $\rho_\Lambda \propto H$ , leading to a constant-rate creation of cold dark matter. We derive all relevant expressions to calculate the mass function and the cluster number density using the Sheth–Tormann formalism and show that the effect of the interaction process is to increase the number of bound structures of large masses ( $M \gtrsim 10^{14} M_\odot h^{-1}$ ) when compared to the standard  $\Lambda$  cold dark matter model. Since these models are not reducible to each other, this number counts signature can in principle be tested in future surveys.

**Key words:** cosmological parameters – dark energy – distance scale – large-scale structure of Universe.

## 1 INTRODUCTION

With the accumulation of high-quality cosmological data from Type Ia supernovae (SNe Ia) observations, anisotropies in the cosmic microwave background (CMB) and measurements of the large-scale properties of the Universe (LSS), the need for an acceleration mechanism governing the late-time cosmic evolution has been confirmed (Sahni & Starobinsky 2000; Padmanabhan 2003; Peebles & Ratra 2003; Alcaniz 2006; Copeland, Sami & Tsujikawa 2006; Frieman 2008). From the observational viewpoint, the standard  $\Lambda$ CDM model, whose cosmic dynamics is driven by a cosmological constant  $\Lambda$  and a component of cold dark matter (CDM), remains as the most consistent cosmological setting. However, despite its observational successes, the standard model suffers from fundamental theoretical issues (see e.g. Weinberg 1986; Sahni & Starobinsky 2000), which motivate the investigation of various alternative scenarios such as quintessence (Ratra & Peebles 1988; Caldwell, Dave & Steinhardt 1998; Liddle & Scherrer 1999; Steinhardt, Wang & Zlatev 1999), modified gravity theories (Carroll et al. 2004; Capozziello, Cardone & Troisi 2005; Amendola, Polarski & Tsujikawa 2007; Fay, Nesseris & Perivolaropoulos 2007; Santos et al. 2007), decaying vacuum models (Bertolami 1986; Ozer & Taha 1986, 1987; Freese et al. 1987; Carvalho, Lima & Waga 1992; Alcaniz & Lima 2005; Shapiro & Sola 2009; Costa & Alcaniz 2010), among others (see Padmanabhan 2003; Peebles & Ratra 2003; Alcaniz 2006; Copeland et al. 2006; Frieman 2008 and references therein).

The implementation of observational tests that are able to distinguish between such scenarios and the standard one has become one of the most important tasks nowadays in cosmology since they not only test the observational viability of these alternative models but

also discuss the standard cosmology in a more general perspective. However, many of these models behave very similarly to the standard  $\Lambda$ CDM paradigm at the level of background evolution, making it difficult to distinguish them through observational data such as SNe Ia measurements. This forces us to go beyond the background expansion, i.e. towards perturbations and the non-linear regime of structure formation. In this regard, observation of cluster number counts as function of the cluster mass and redshift have been accounted as a potential candidate for probing both the expansion rate and the growth of perturbations, thereby providing independent constraints on cosmological parameters, such as the present-day matter density parameter  $\Omega_{m0}$  and the rms density fluctuation  $\sigma_8$ . This kind of data can, therefore, provide a new window for cosmological modelling, with the ability of distinguishing between the various dark energy models or among the various alternative scenarios by their effects on structure formation. It is also worth mentioning that there are a number of surveys, either ongoing or being planned for the near future, that are expected to release a large number of cluster counts data. This certainly will improve the complementarity of cluster observations with other cosmological probes, such as CMB, SNe Ia and LSS observations.

In this paper, we study the non-linear evolution of density perturbations in a spatially flat cosmological model in which vacuum decays linearly with the Hubble parameter, leading to the production of CDM at a constant rate (Borges & Carneiro 2005). This is a particular case of models with interaction in the dark sector (Zimdahl et al. 2001; Costa, Alcaniz & Maia 2008; Jesus et al. 2008; Wu et al. 2008; del Campo, Herrera & Pavón 2009; Koyama, Maartens & Song 2009; Chimento 2010; He, Wang & Abdalla 2011; Wands, De-Santiago & Wang 2012) that has been shown competitive, with good concordance in both background and linear perturbation levels (Carneiro et al. 2006, 2008; Borges et al. 2008; Pigozzo et al. 2011; Alcaniz et al. 2012; Velten, Montiel & Carneiro 2013). Further, we

\* E-mail: [alcaniz@on.br](mailto:alcaniz@on.br)

analyse how such an interacting process affects the predicted halo abundance. For this purpose we calculate all relevant expressions for the mass function and the cluster number density following the Sheth–Torman formalism (Sheth & Torman 1999) and compare our results with that of the standard  $\Lambda$ CDM scenario. We also test the robustness of our results by considering a mass function different from the one introduced by Sheth–Torman. The structure of the paper is as follows. In Section 2, we introduce the decaying vacuum model and discuss the background evolution. In Section 3, we study non-linear density perturbations through the spherical collapse model. We calculate the number density as function of the cluster mass using the Sheth–Torman formalism in Section 4 and finally we discuss our main results in Section 5. We are using  $8\pi G = c = 1$  in this paper.

## 2 BACKGROUND

We consider a Friedmann–Lemaître–Robertson–Walker (FLRW) cosmology in which there is a continuous decay of vacuum energy into dark matter. In other words, the dark sector consists of CDM interacting with a varying dark energy component with equation-of-state parameter  $\omega = -1$ . Owing to this interaction, total energy conservation is expressed by the continuity equation as

$$\dot{\rho}_m + 3\frac{\dot{a}}{a}\rho_m = -\dot{\rho}_\Lambda, \quad (1)$$

where  $\rho_m$  and  $\rho_\Lambda$  are the energy densities of CDM and vacuum, respectively, and the Friedmann equation reads

$$3H^2(a) \equiv \left(\frac{\dot{a}}{a}\right)^2 = \rho_m + \rho_\Lambda. \quad (2)$$

Some possible forms of the time-dependent vacuum have been investigated in the literature (Bertolami 1986; Ozer & Taha 1986, 1987; Freese et al. 1987; Carvalho et al. 1992; Alcaniz & Lima 2005; Shapiro & Sola 2009; Costa & Alcaniz 2010). In this paper, we consider a particular ansatz  $\rho_\Lambda \propto H(a)$ , which corresponds to a constant-rate CDM creation from vacuum (Borges & Carneiro 2005). With this ansatz we derive the Hubble expansion as a function of the redshift as

$$H(z) = H_0[1 - \Omega_{m0} + \Omega_{m0}(1+z)^{3/2}]. \quad (3)$$

Since matter is no longer conserved, it does not evolve as  $\rho_m(z) = 3H_0^2\Omega_{m0}(1+z)^3$  as in the standard model, but rather as

$$\rho_m(z) = 3H_0^2\Omega_{m0} [\Omega_{m0}(1+z)^3 + (1 - \Omega_{m0})(1+z)^{3/2}]. \quad (4)$$

The second term on the right-hand side of equation (4) results from dark matter creation. At high redshifts, the above scaling relation reduces to

$$\rho_m(z) = 3H_0^2\Omega_{m0}^2(1+z)^3 \quad (z \gg 1), \quad (5)$$

where the extra factor  $\Omega_{m0}$  means that, for the same amount of matter at high- $z$ , the decaying model predicts a larger amount at present when compared to the  $\Lambda$ CDM model. In fact, the test of this model against observations of the matter linear power spectrum led to  $\Omega_{m0} \approx 0.45$  (Borges et al. 2008; Alcaniz et al. 2012). This value is in good agreement with results from background observations, namely the Hubble diagram for SN Ia, the position of the first acoustic peak in the CMB anisotropy spectrum, and baryonic acoustic oscillations (BAO) data (Pigozzo et al. 2011). For a more detailed discussion on the current observational constraints on this class of models, we refer the reader to Alcaniz et al. (2012).

## 3 EVOLUTION OF MATTER PERTURBATIONS

In this section, we analyse the basic equations required to study the behaviour of matter perturbations within the framework of the above discussed cosmological model. Let us start with the equations for energy conservation, momentum conservation and the gravitational field,

$$\frac{\partial \rho}{\partial t} + \nabla_r \cdot (\rho \mathbf{u}) + p \nabla_r \cdot \mathbf{u} = 0, \quad (6)$$

$$\frac{\partial \mathbf{u}}{\partial t} + (\mathbf{u} \cdot \nabla_r) \mathbf{u} = -\nabla_r \phi - \frac{\nabla_r p}{\rho + p}, \quad (7)$$

$$\nabla_r^2 \phi = \frac{\rho + 3p}{2}, \quad (8)$$

where  $\rho$ ,  $p$ ,  $\mathbf{u}$  and  $\phi$  are, respectively, the energy density, pressure, velocity and gravitational potential of the cosmic fluid. Introducing the cosmological perturbations

$$\rho_m(\mathbf{r}, t) = \rho_m(t) + \delta\rho_m(\mathbf{r}, t), \quad (9)$$

$$\mathbf{u}(\mathbf{r}, t) = \mathbf{u}_0(t) + \mathbf{v}(\mathbf{r}, t), \quad (10)$$

$$\phi(\mathbf{r}, t) = \phi_0(t) + \Phi(\mathbf{r}, t) \quad (11)$$

into the set of equations (6)–(8), we obtain

$$\delta\dot{\rho}_m + 3H\delta\rho_m + \rho_m \nabla_r \cdot \mathbf{v} + (\nabla_r \cdot \mathbf{v})\delta\rho_m + (H\mathbf{r} + \mathbf{v}) \cdot \nabla_r \delta\rho_m = 0, \quad (12)$$

$$\dot{\mathbf{v}} + H(\mathbf{r} \cdot \nabla_r)\mathbf{v} + H\mathbf{v} + (\mathbf{v} \cdot \nabla_r)\mathbf{v} + \nabla_r \Phi = 0, \quad (13)$$

$$\nabla_r^2 \Phi = \frac{\delta\rho_m}{2}, \quad (14)$$

where  $\mathbf{u}_0 = H\mathbf{r}$  corresponds to the Hubble flow and  $\mathbf{v}$  corresponds to the matter peculiar velocities. Here we have taken  $\delta\rho_\Lambda = 0$ , which is valid for the model discussed in Section 2 when one considers modes well inside the horizon (Zimdahl et al. 2011). Generally, in the spherical collapse model we assume a homogeneous distribution of matter within a sphere of radius  $\mathbf{r} = a(t)\mathbf{x}$ , so the term  $\nabla_r \delta\rho_m$  appearing in the energy conservation equation is null. Furthermore, to maintain a spherically symmetric profile we choose a velocity field of type  $\mathbf{v} = \theta\mathbf{x}/3$ , with  $\nabla_r \cdot \mathbf{v} = \theta$ . We then use the definition of the density contrast  $\delta_m = \delta\rho_m/\rho_m$  and change to comoving variables, with  $\nabla_r = \nabla/a$ . Hence, equations (12) and (13) are rewritten as

$$\dot{\delta}_m = -\frac{\Psi}{\rho_m}\delta_m - \frac{\theta}{a}(1 + \delta_m), \quad (15)$$

$$\dot{\theta} + H\theta + \frac{\theta^2}{3a} = -\frac{a\rho_m\delta_m}{2}, \quad (16)$$

where  $\Psi = -\dot{\rho}_\Lambda$ . Differentiating (15) with respect to cosmic time and eliminating  $\theta$  and  $\dot{\theta}$ , we obtain a second-order non-linear differential equation for the matter density contrast,

$$\begin{aligned} \ddot{\delta}_m + \left(2H + \frac{\Psi}{\rho_m}\right)\dot{\delta}_m \\ + \left[\frac{d}{dt}\left(\frac{\Psi}{\rho_m}\right) + 2H\frac{\Psi}{\rho_m} - \frac{\rho_m(1 + \delta_m)}{2}\right]\delta_m \\ = \frac{1}{3(1 + \delta_m)}\left(4\dot{\delta}_m^2 + \frac{5\Psi}{\rho_m}\delta_m\dot{\delta}_m + \frac{\Psi^2}{\rho_m^2}\delta_m^2\right). \end{aligned} \quad (17)$$

The corresponding linear equation is obtained for  $\delta_m \ll 1$  and is given by (Arcuri & Waga 1994; Borges et al. 2008)

$$\ddot{\delta}_m + \left(2H + \frac{\Psi}{\rho_m}\right) \dot{\delta}_m + \left[\frac{d}{dt} \left(\frac{\Psi}{\rho_m}\right) + 2H \frac{\Psi}{\rho_m} - \frac{\rho_m}{2}\right] \delta_m = 0. \quad (18)$$

Changing variables from  $t$  to redshift  $z$ , the evolution equation (17) takes the form

$$H^2(1+z)^2 \delta_m'' - \left[f(z)(1+z)^2 + H(1+z) \frac{\Psi}{\rho_m}\right] \delta_m' + \left[2H \frac{\Psi}{\rho_m} - \frac{1}{2} \rho_m (1 + \delta_m)\right] \delta_m = \frac{4}{3} H^2 (1+z)^2 \frac{\delta_m'^2}{1 + \delta_m} - \frac{5}{3} H(1+z) \frac{\Psi}{\rho_m} \frac{\delta_m \delta_m'}{1 + \delta_m} + \frac{1}{3} \left(\frac{\Psi}{\rho_m}\right)^2 \frac{\delta_m^2}{1 + \delta_m}, \quad (19)$$

where the background functions are given by equations (3) and (4) and

$$\frac{\Psi}{\rho_m} = \frac{3H_0}{2} (1 - \Omega_{m0}), \quad (20a)$$

$$f(z) = -\frac{H_0^2}{2} (1+z)^{-1} [2\Omega_{m0} + \Omega_{m0}(1+z)^{3/2} - 2] \times [1 - \Omega_{m0} + \Omega_{m0}(1+z)^{3/2}]. \quad (20b)$$

#### 4 NUMBER COUNTS

In this section we study the imprint of the particle creation process described above on the predicted abundance of bound objects, such as clusters and groups of galaxies. The formation of these structures can be understood by the spherical top-hat model, in which density perturbations initially increase linearly with the scale factor in the matter dominated phase, according to equation (18). Once the overdensity exceeds a critical value  $\delta_c$ , it decouples from the Hubble flow, reaches to a maximum radius and then starts collapsing under its own gravitational force until its virialization to a bound structure. The critical density contrast  $\delta_c$  is a model-dependent quantity and we calculate it for the model of Section 2 as follows (Abramo et al. 2007; Pace, Waizmann & Bartelman 2010; Campanelli et al. 2012). First, we integrate the non-linear equation (17), looking for the initial conditions for which  $\delta_m$  diverges at some redshift  $z_c$ . Using these same initial conditions we integrate the linear equation (18) to obtain  $\delta_c(z_c)$ . We also obtain the linear growth function solving equation (18) with the initial conditions  $\delta_i \sim a_i$  and  $\delta_i' \sim 1$  at some initial  $a_i$  (say, at the epoch of matter-radiation equality).

The comoving number density of collapsed objects at redshift  $z$  within the mass interval  $M$  and  $M + dM$  is given by

$$\frac{dn(M, z)}{dM} = -\frac{\bar{\rho}_m}{M} \frac{d \ln \sigma(M, z)}{dM} f(\sigma), \quad (21)$$

where  $\bar{\rho}_m$  is the comoving background density,  $\sigma(z)$  represents the variance of the linear density field on a given comoving scale  $R$  and  $f(\sigma)$  is the mass function. Note that in the  $\Lambda$ CDM case  $\bar{\rho}_m$  is equal to the present density  $\rho_{m0}$ , but, owing to equation (4), for the interacting model discussed here it is given by  $\bar{\rho}_m = \rho_{m0} \beta(z)$ , with  $\beta(z) = \Omega_{m0} + (1 - \Omega_{m0})(1+z)^{-3/2}$ . In what concerns the mass function, it is well known that the Press–Schechter formalism (Press & Schechter 1974) presents over (under) predictions at the low (high) mass limit when compared with numerical simulations. Thus, other mass functions  $f(\sigma)$  have been proposed in the literature

(see e.g. Sheth & Torman 1999; Jenkins et al. 2001; Reed et al. 2003, 2007; Tinker et al. 2008). In our analysis we use a modified form of the Press–Schechter mass function, the so-called Sheth & Torman mass function, which is motivated by the ellipsoidal collapse of overdense regions and is more compatible with present-day simulations. It reads as (Sheth & Torman 1999)

$$f(\sigma) = A \sqrt{\frac{2q}{\pi}} \left[1 + \left(\frac{\sigma^2(z)}{q \delta_c^2(z)}\right)^p\right] \frac{\delta_c(z)}{\sigma(z)} \exp\left[-\frac{\delta_c^2(z) q}{2\sigma^2(z)}\right], \quad (22)$$

where  $A$  is a normalization constant. Values of  $(p, q)$  equal to  $(0, 1)$  recover the Press–Schechter mass function, whose shape and amplitude are motivated by the spherical (rather than ellipsoidal) collapse of matter overdensities. The values  $p = 0.3$  and  $q = 0.707$  correspond to an accurate fitting of the  $\Lambda$ CDM model with  $N$ -body simulations (Sheth & Torman 1999).

The variance  $\sigma(z)$  can be written as (Bond et al. 1991; Peebles 1993; Eke, Cole & Frenk 1996; Dodelson 2003)

$$\sigma^2(R, z) = \frac{D^2(z)}{2\pi^2} \int_0^\infty k^2 P(k) W^2(kR) dk, \quad (23)$$

with a corresponding mass  $M = \frac{4\pi}{3} \rho_{m0} R^3 \beta(z)$  instead of the standard-case  $M = \frac{4\pi}{3} \rho_{m0} R^3$ . The growth function  $D(z) = \delta(z)/\delta(0)$  is normalized such that  $D(z) = 1$  at present.  $W(kR)$  is the Fourier transform of a spherical top-hat filter of radius  $R$ , i.e.  $W(kR) = 3(\sin(kR)/(kR)^3 - \cos(kR)/(kR)^2)$ . The CDM power spectrum is given by  $P(k) = P_0 k^{n_s} T^2(k)$ , where  $T(k)$  is the transfer function. We use the BBKS transfer function (Bardeen et al. 1986; Martin, Riazuelo & Sakellariadou 2000) which, for a baryon density parameter  $\Omega_{b0} \ll \Omega_{m0}$ , can be approximated by

$$T(x = k/k_{\text{eq}}) = \frac{\ln[1 + 0.171x]}{(0.171x)} \times [1 + 0.284x + (1.18x)^2 + (0.399x)^3 + (0.490x)^4]^{-0.25}, \quad (24)$$

where  $k_{\text{eq}}^{-1}$  is the comoving Hubble scale at the redshift of matter-radiation equality. Note that, because of the matter density scaling (5), for the decaying vacuum model we obtain  $k_{\text{eq}} = 0.073 h^2 \Omega_{m0}^2 \text{Mpc}^{-1}$  instead of the standard result  $k_{\text{eq}} = 0.073 h^2 \Omega_{m0} \text{Mpc}^{-1}$  (we set the present-day radiation density parameter as  $\Omega_{R0} = 4.15 \times 10^{-5} h^{-2}$ ). The normalization of the power spectrum is done in terms of  $\sigma_8$ , the present rms fluctuation at a scale of  $8h^{-1} \text{Mpc}$ . With this, the expression for  $\sigma^2(M, z)$  becomes

$$\sigma^2(M, z) = \sigma_8^2 \frac{D^2(z)}{D_\Lambda^2(0)} \frac{\int_0^\infty k^{n_s+2} T^2(\Omega_{m0\Lambda}, k) W^2(kR) dk}{\int_0^\infty k^{n_s+2} T_\Lambda^2(\Omega_{m0\Lambda}, k) W^2(kR_8) dk}, \quad (25)$$

where the index  $\Lambda$  stands for the  $\Lambda$ CDM model. We set  $\sigma_8 = 0.83$ ,  $h = 0.67$  and  $n_s = 0.971$ , as given by the Planck Collaboration XVI (2014). It is worth mentioning that, for our interacting scenario, the concordance value of the matter density parameter obtained from a joint analysis involving CMB, SNe Ia, BAO and the linear power spectrum is about  $\Omega_{m0} = 0.45$  (Borges et al. 2008; Carneiro et al. 2006, 2008; Pigozzo et al. 2011; Alcaniz et al. 2012). We will use this value in the further analyses of this model, whereas for the  $\Lambda$ CDM case we fix the matter density parameter at  $\Omega_{m0\Lambda} = 0.3$ .

#### 5 DISCUSSION

In Figs 1(a) and (b) (upper panels) we show the comoving number density as function of the mass  $M$  for  $z = 0$  and  $z = 1$ , respectively. In both cases, the interacting model predicts approximately the same number density as the standard model for cluster masses below

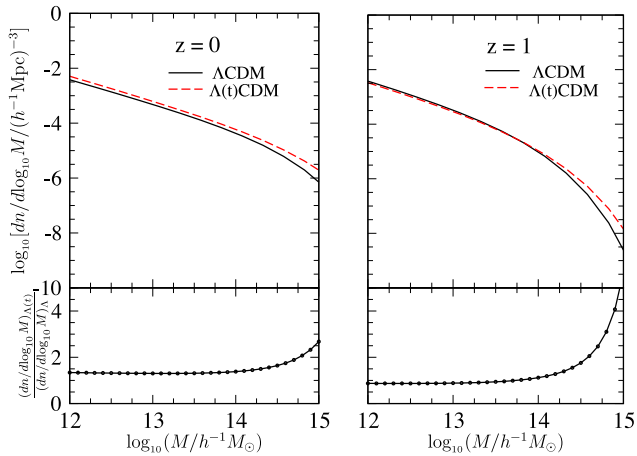


**Figure 1.** Upper panels: the comoving number density as a function of mass for the decaying vacuum and the standard  $\Lambda$ CDM model at redshifts  $z = 0$  and  $z = 1$ , respectively. Lower panels: corresponding differences in the comoving number density with respect to the standard  $\Lambda$ CDM model.

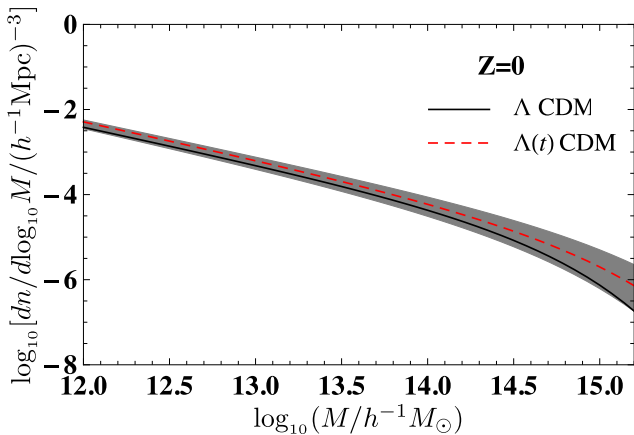


**Figure 2.** Variation of the comoving number density with respect to mass for the decaying vacuum (dashed line) and the standard  $\Lambda$ CDM model (solid line). The shadowed region corresponds to the comoving number density of the decaying vacuum model when the Sheth–Torman parameters ( $p$ ,  $q$ ) vary about 30 per cent from their standard values.

$M = 10^{14} M_{\odot}$ . The corresponding differences in the number density with respect to the  $\Lambda$ CDM case are depicted in the lower panels of Fig. 1. We find that the predicted  $dn/dM$  difference between these scenarios increases considerably for  $M > 10^{14} M_{\odot}$ , reaching  $\sim 38$  per cent and  $\sim 64$  per cent, respectively, for  $M = 10^{14} M_{\odot} h^{-1}$  and  $M = 10^{14.5} M_{\odot} h^{-1}$  at  $z = 0$  and  $\sim 12$  per cent and  $\sim 74$  per cent at  $z = 1$ . This is an important result since ongoing and planned surveys, like *eROSITA* (Merloni et al. 2012; Pillepich, Porciani & Reiprich 2012) and J-PAS (Benítez et al. 2014), must be able to detect such differences and, therefore, to distinguish between this class of interacting cosmology and the  $\Lambda$ CDM model.

As mentioned earlier, the predicted behaviour of  $dn/dM$  depends on the values of the parameters  $p$  and  $q$  (see equation 22). In order to better visualize this dependence, we show in Fig. 2 the expected change in the evolution of the comoving number density considering different values of the pair ( $p$ ,  $q$ ) within a 30 per cent interval (grey region) from the standard values  $p = 0.707$  and  $q = 0.3$  discussed in the previous section (red dashed line). We find that larger values of  $p$  and  $q$  moves the interacting model prediction towards the standard result. For completeness, we also tested the dependence of

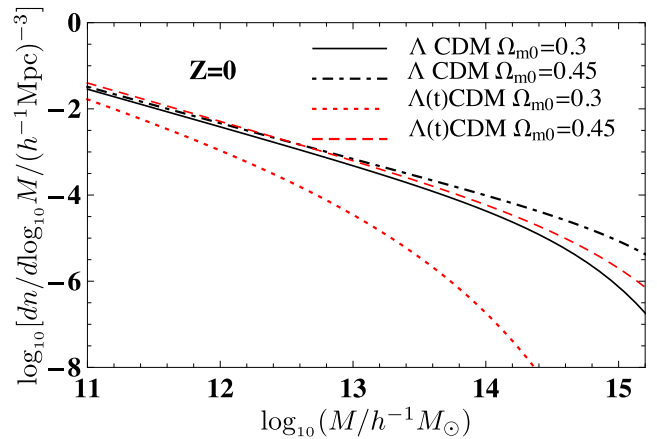


**Figure 3.** Comoving number density for the standard  $\Lambda$ CDM and the interacting models with different values of the matter density parameters.

these results with the Sheth–Torman mass function by repeating our calculations using the mass function introduced in Reed et al. (2003, 2007). No significant difference from the results shown in Fig. 1 was found. From these results, we conclude that the main difference in cluster number density between the  $\Lambda$ CDM and interacting models is due to the dynamical behaviour of the models instead of the mass function used in the number counts calculations. The reader may also ask whether the small difference between the predictions of the two models is just due to the different best-fitting values of the matter density parameter,  $\Omega_{m0} = 0.3$  for the standard model and  $\Omega_{m0} = 0.45$  for the interacting model. An inspection of equation (25), however, shows that this is not the case. For the  $\Lambda$ CDM model, a change in  $\Omega_{m0}$  from 0.3 to 0.45 leads indeed to a small difference in the number density whereas in the interacting case, the matter density appears squared in the transfer function (24), leading to a larger difference when it is changed from 0.45 to 0.3. This is illustrated in Fig. 3.

## 6 FINAL REMARKS

The nature of the cosmological dark sector is certainly one of the main open problems of modern cosmology. A residual  $\Lambda$  term, although in good agreement with current observations, exacerbates the well-known cosmological constant problems (Weinberg 1986), requiring a natural explanation for its small value. In this paper, we have discussed the ability of cluster number counts to constrain a class of alternative scenarios in which the vacuum energy density decays linearly with the Hubble parameter  $H$ . This particular class of  $\Lambda(t)$ CDM models has been tested against precise background observations, namely the position of the first peak of the CMB anisotropy spectrum, the Hubble diagram for SNe Ia and the BAO distance scale (Carneiro et al. 2006, 2008; Pigozzo et al. 2011) and also provides a good fit to the linear power spectrum of matter (Borges et al. 2008). It is worth mentioning that a joint analysis of these observations has led to a remarkable concordance, with  $\Omega_{m0} \approx 0.45$  (Alcaniz et al. 2012), which is the matter density value used to perform the present results.

We have studied the structure formation in these  $\Lambda(t)$ CDM scenarios and derived all relevant expressions to calculate the mass function and the cluster number density using the Sheth–Torman formalism. We have found that the cluster counts prediction of the  $\Lambda$ CDM and  $\Lambda(t)$ CDM models are approximately the same for cluster masses below  $M = 10^{14}$  solar masses and becomes different

for larger values of  $M$  and higher  $z$ . Such differences, however, are not large enough to be confronted to current observations but may be detected by ongoing and planned surveys capable to observe high-mass galaxy clusters at higher redshifts (e.g. *eROSITA*, Merloni et al. 2012; Pillepich et al. 2012; and J-PAS, Benitez et al. 2014). We have also studied the dependence of our results on the Sheth–Torman mass function by performing a similar analysis with the mass function introduced in Reed et al. (2003, 2007). We have found no significant difference in the results, which makes them robust. A quantitative comparison of these models predictions with the current cluster number observations and mock data from ongoing surveys is the subject of a forthcoming publication.

## ACKNOWLEDGEMENTS

The authors thank T. Roy Choudhury for helpful discussions. This work is partially supported by CNPq, FAPERJ, FAPESB and INEspaço.

## REFERENCES

- Abramo L. R., Batista R. C., Liberato L., Rosenfeld R., 2007, *J. Cosmol. Astropart. Phys.*, 0711, 012
- Alcaniz J. S., 2006, *Braz. J. Phys.*, 36, 1109
- Alcaniz J. S., Lima J. A. S., 2005, *Phys. Rev. D*, 72, 063516
- Alcaniz J. S., Borges H. A., Carneiro S., Fabris J. C., Pigozzo C., Zimdahl W., 2012, *Phys. Lett. B*, 716, 165
- Amendola L., Polarski D., Tsujikawa S., 2007, *Phys. Rev. Lett.*, 98, 131302
- Arcuri R. C., Waga I., 1994, *Phys. Rev. D*, 50, 2928
- Bardeen J. M., Bond J. R., Kaiser N., Szalay A. S., 1986, *ApJ*, 304, 15
- Benitez N. et al., 2014, preprint ([arXiv:1403.5237](https://arxiv.org/abs/1403.5237))
- Bertolami O., 1986, *Nuovo Cimento*, 93, 36
- Bond J. R., Cole S., Efstathiou G., Kaiser N., 1991, *ApJ*, 379, 440
- Borges H. A., Carneiro S., 2005, *Gen. Relativ. Gravit.*, 37, 1385
- Borges H. A., Carneiro S., Fabris J. C., Pigozzo C., 2008, *Phys. Rev. D*, 77, 043513
- Caldwell R. R., Dave R., Steinhardt P. J., 1998, *Phys. Rev. Lett.*, 80, 1582
- Campanelli L., Fogli G. L., Kahnashvili T., Marrone A., Bharat Ratra, 2012, *Eur. Phys. J. C*, 72, 2218
- Capozziello S., Cardone V. F., Troisi A., 2005, *Phys. Rev. D*, 71, 043503
- Carneiro S., Borges H. A., Pigozzo C., Alcaniz J. S., 2006, *Phys. Rev. D*, 74, 023532
- Carneiro S., Dantas M. A., Pigozzo C., Alcaniz J. S., 2008, *Phys. Rev. D*, 77, 083504
- Carroll S. M., Duvvuri V., Trodden M., Turner M. S., 2004, *Phys. Rev. D*, 70, 043528
- Carvalho J. C., Lima J. A. S., Waga I., 1992, *Phys. Rev. D*, 46, 2404
- Chimento L. P., 2010, *Phys. Rev. D*, 81, 04352
- Copeland E. J., Sami M., Tsujikawa S., 2006, *Int. J. Mod. Phys. D*, 15, 1753
- Costa F. E. M., Alcaniz J. S., 2010, *Phys. Rev. D*, 81, 043506
- Costa F. E. M., Alcaniz J. S., Maia J. M. F., 2008, *Phys. Rev. D*, 77, 083516
- del Campo S., Herrera R., Pavón D., 2009, *J. Cosmol. Astropart. Phys.*, 0901, 020
- Dodelson S., 2003, *Modern Cosmology*. Academic Press, New York
- Eke V. R., Cole S., Frenk C. S., 1996, *MNRAS*, 282, 263
- Fay S., Nesseris S., Perivolaropoulos L., 2007, *Phys. Rev. D*, 76, 063504
- Freese K., Adams F. C., Frieman J. A., Mottola E., 1987, *Nucl. Phys. B*, 287, 797
- Frieman J. A., 2008, in Pellegrini P., Daflon S., Alcaniz J., Telles E., eds, *AIP Conf. Proc. Vol. 1057, Graduate School in Astronomy: XII Special Courses at the National Observatory of Rio de Janeiro*. Am. Inst. Phys., New York, p. 87
- He J. H., Wang B., Abdalla E., 2011, *Phys. Rev. D*, 83, 063515
- Jenkins A., Frenk C. S., White S. D. M., Colberg J. M., Cole S., Evrard A. E., Couchman H. M. P., Yoshida N., 2001, *MNRAS*, 321, 372
- Jesus J. F., Santos R. C., Alcaniz J. S., Lima J. A. S., 2008, *Phys. Rev. D*, 78, 063514
- Koyama K., Maartens R., Song Y. S., 2009, *J. Cosmol. Astropart. Phys.*, 0910, 017
- Liddle A. R., Scherrer R. J., 1999, *Phys. Rev. D*, 59, 023509
- Martin J., Riazuelo A., Sakellariadou M., 2000, *Phys. Rev. D*, 61, 083518
- Merloni A. et al., 2012, preprint ([arXiv:1209.3114](https://arxiv.org/abs/1209.3114))
- Ozer M., Taha M. O., 1986, *Phys. Lett.*, 171, 363
- Ozer M., Taha M. O., 1987, *Nucl. Phys. B*, 287, 776
- Pace F., Waizmann J.-C., Bartelman M., 2010, *MNRAS*, 406, 1865
- Padmanabhan T., 2003, *Phys. Rept.*, 380, 235
- Peebles P. J. E., 1993, *Principles of Physical Cosmology*. Princeton Univ. Press, Princeton, NJ
- Peebles P. J. E., Ratra B., 2003, *Rev. Mod. Phys.*, 75, 559
- Pigozzo C., Dantas M. A., Carneiro S., Alcaniz J. S., 2011, *J. Cosmol. Astropart. Phys.*, 1108, 022
- Pillepich A., Porciani C., Reiprich T. H., 2012, *MNRAS*, 422, 44
- Planck Collaboration XVI, 2014, *A&A*, 571, 66
- Press W. H., Schechter P., 1974, *ApJ*, 187, 425
- Ratra B., Peebles P. J. E., 1988, *Phys. Rev. D*, 37, 3406
- Reed D., Gardner J., Quinn T., Stadel J., Fardal M., Lake G., Governato F., 2003, *MNRAS*, 346, 565
- Reed D., Bower R., Frenk C., Jenkins A., Theuns T., 2007, *MNRAS*, 374, 2
- Sahni V., Starobinsky A., 2000, *Int. J. Mod. Phys. D*, 9, 373
- Santos J., Alcaniz J. S., Rebouas M. J., Carvalho F. C., 2007, *Phys. Rev. D*, 76, 083513
- Shapiro I. L., Sola J., 2009, *Phys. Lett. B*, 682, 105
- Sheth R. K., Torman G., 1999, *MNRAS*, 308, 119
- Steinhardt P. J., Wang L., Zlatev I., 1999, *Phys. Rev. D*, 59, 123504
- Tinker J. A., Kravtsov A. V., Klypin A., Abazajian K., Warren M., Yepes G., Gottlber S., Holz D. E., 2008, *ApJ*, 688, 709
- Velten H., Montiel A., Carneiro S., 2013, *MNRAS*, 431, 3301
- Wands D., De-Santiago J., Wang Y., 2012, *Classical Quantum Gravity*, 29, 145017
- Weinberg S., 1986, *Rev. Mod. Phys.*, 61, 1
- Wu Q., Gong Y., Wang A., Alcaniz J. S., 2008, *Phys. Lett. B*, 659, 34
- Zimdahl W., Schwarz D. J., Balakin A. B., Pavón D., 2001, *Phys. Rev. D*, 64, 063501
- Zimdahl W., Borges H. A., Carneiro S., Fabris J. C., 2011, *J. Cosmol. Astropart. Phys.*, 1104, 028

This paper has been typeset from a  $\text{\TeX}/\text{\LaTeX}$  file prepared by the author.